Virus Research 201 (2015) 101–112

Contents lists available at ScienceDirect

Virus Research

journal homepage: www.elsevier.com/locate/virusres

Phylogenetic and phylogeographic mapping of the avian coronavirus spike protein-encoding gene in wild and synanthropic birds

Ricardo Durães-Carvalho[a,b,*], Leonardo C. Caserta[a], Ana C.S. Barnabé[a], Matheus C. Martini[a], Paulo V.M. Simas[a], Márcia M.B. Santos[c], Marco Salemi[b], Clarice W. Arns[a,*]

[a] Laboratory of Virology, Department of Genetics, Evolution and Bioagents, University of Campinas (UNICAMP), São Paulo, Brazil
[b] Emerging Pathogens Institute & Department of Pathology, Immunology and Laboratory Medicine, University of Florida, Gainesville, FL, USA
[c] Department of Biological Sciences, Federal University of Juiz de Fora, Minas Gerais, Brazil

ARTICLE INFO

Article history:
Received 10 January 2015
Received in revised form 2 March 2015
Accepted 4 March 2015
Available online 11 March 2015

Keywords:
Avian coronaviruses
Phylogeny
Bayesian phylogeography

ABSTRACT

The evolution and population dynamics of avian coronaviruses (AvCoVs) remain underexplored. In the present study, in-depth phylogenetic and Bayesian phylogeographic studies were conducted to investigate the evolutionary dynamics of AvCoVs detected in wild and synanthropic birds. A total of 500 samples, including tracheal and cloacal swabs collected from 312 wild birds belonging to 42 species, were analysed using molecular assays. A total of 65 samples (13%) from 22 bird species were positive for AvCoV. Molecular evolution analyses revealed that the sequences from samples collected in Brazil did not cluster with any of the AvCoV S1 gene sequences deposited in the GenBank database. Bayesian framework analysis estimated an AvCoV strain from Sweden (1999) as the most recent common ancestor of the AvCoVs detected in this study. Furthermore, the analysis inferred an increase in the AvCoV dynamic demographic population in different wild and synanthropic bird species, suggesting that birds may be potential new hosts responsible for spreading this virus.

1. Introduction

Avian coronaviruses (AvCoVs) are enveloped viruses with pleomorphic spherical forms belonging to the order *Nidovirales*, family *Coronaviridae*, subfamily *Coronavirinae* and grouped into the *Gamma-CoV* genus (Carstens, 2010). The AvCoV genome consists of positive-sense single-stranded RNA with an approximate size of 27 kb (Jackwood et al., 2012). The genome is subdivided into nine open reading frames (ORFs) that encode a set of non-structural proteins known as the transcriptase–replicase complex, which functions as the RNA polymerase (Pol-1a, -1b) and four main structural proteins (spike surface glycoprotein (S), membrane (M), envelope (E), and nucleocapsid (N)) (Fauquet et al., 2005; Mardani et al., 2008; Mo et al., 2013).

Among the AvCoVs, we highlight Avian infectious bronchitis virus (AIBV), the aetiological agent of infectious bronchitis, which is one of the most important viral diseases in countries with intensive poultry industries (Cavanagh and Gelb, 2008; Jones, 2010), as well as AvCoVs (IBV-like) that were recently detected in several bird orders, such as *Galliformes*, *Anseriformes*, *Columbiformes*, *Charadriiformes*, *Passeriformes*, *Pelacaniformes*, *Ciconiiformes* and *Psittaciformes*, which may influence strongly AvCoV epidemiology (Domanska-Blicharz et al., 2014).

Due to its highly mutagenic character, the control of AvCoVs is a constant challenge for the poultry industry. The evolutionary dynamics of AvCoVs are characterised by the continuous emergence of new variants, resulting in multiple serotypes that do not confer cross-protective immunity to each other (Jackwood et al., 2012). AvCoV diversity is mainly driven by three factors: the elevated mutation rate of the RNA-dependent RNA polymerase; the great diversity of birds, which provides many potential target hosts for different AvCoV genotypes; and the facilitation of viral transmission and dissemination across large geographic areas and between different species by bird migration and flock lifestyles (Keesing et al., 2010). These factors have driven the generation of a wide

* Corresponding authors at: Laboratory of Virology, Institute of Biology, P.O. Box: 6109, University of Campinas – UNICAMP, 13083-970, Campinas-SP, Brazil. Tel.: +55 19 3521 6258.
E-mail addresses: rdcarval@gmail.com (R. Durães-Carvalho), clarns@gmail.com (C.W. Arns).

http://dx.doi.org/10.1016/j.virusres.2015.03.002
0168-1702/

variety of AvCoV variants, resulting in persistent reservoirs that can become relevant for human populations when wild animals acquire synanthropic habits and start to live in close proximity to domesticated poultry (Jourdain et al., 2007; Felippe et al., 2010).

Despite the health and economic importance of AvCoVs to the poultry industry, knowledge about the prevalence and distribution of these viruses in wild and synanthropic birds remains limited. The variety of potentially infected bird species and the annual use of intercontinental territory by migratory birds increase the risk of the introduction and spread of new pathogens and new variants of CoV (Jourdain et al., 2007; Somveille et al., 2013), requiring the development of new analytical methods.

Phylogenetic inferences are extremely useful tools for the study of the molecular ecoepidemiology of pathogens and for the elucidation of epidemiologically important characteristics. Phylogenetic inferences enable the molecular characterisation of existing variants and the discovery of new viral variants with potential health repercussions. Furthermore, these techniques permit an analysis of the evolutionary history of new variants (Lemey et al., 2009; Yang and Rannala, 2012).

In addition to providing information on the timeline of evolutionary processes, phylogenetic studies can be used to compare and associate individuals from specific geographical regions with the time of the most recent common ancestor (tMRCA) of each region studied. Tools such as phylogeography provide a useful approach for understanding the origins and distributions of different viral strains to elucidate population evolution dynamics and their dependence on the environment. Phylogeographic techniques have been applied to many viral infections that threaten human health, including dengue, rabies, influenza and HIV (Holmes, 2004; Kühnert et al., 2011), but there is a lack of phylogeographic information regarding CoVs.

This pilot study applied a phylogeographic approach to the evolution of the AvCoV spike protein gene to study the spatial arrangements of different genetic lineages within species and between closely related species, to analyse the principles and processes that determine the geographic distribution of lineages, and to establish a resource for improved molecular characterisation of available and as-yet unidentified AvCoV strains.

2. Material and methods

2.1. Ethical statement

The capture and management of wild and synanthropic animals for the collection of biological samples was performed in accordance with current Authorization and Information System of Biodiversity (SISBIO) recommendations, Brazil, protocol no. 34751-1/12.

2.2. Samples and population study

A total of 500 tracheal and/or cloacal swabs were collected from 42 different bird species belonging to 13 orders (Supplementary Table S1). The biological samples were collected in the cities of Campinas and São Paulo in the State of São Paulo (Southeastern Brazil) and the city of Florianópolis (Southern Brazil) in the State of Santa Catarina between 2006 and 2013. The swabs were placed in 1.5-mL microtubes and identified with the name of the bird species and a specific code. The samples were immediately transported in coolers with ice to the Laboratory of Animal Virology (LVA) at the Institute of Biology at UNICAMP and stored at −80 °C until further processing.

2.3. Route map of migratory and non-migratory birds

The maps showing the birds and their specific routes were derived from the BirdLife International (Cambridge, United Kingdom) and NatureServe (Arlington, United States of America) databases. These maps consist of Geographic Information System (GIS) shapefiles that show the geographic extent and distribution of all bird species investigated in the study (Fig. 1).

2.4. RNA extraction and detection of AvCoVs by qRT-PCR

A total of 500 μL of Minimum Essential Medium (MEM) (Nutricell, Brazil) was added to the microtube containing the swab with the biological sample. The remaining procedure was performed according to the QIAamp® Viral RNA Mini Kit (QIAGEN, CA, USA) manufacturer's instructions.

Each extracted RNA sample was subjected to Real Time RT-qPCR using previously published primers for the 5′-Untranslated Region (UTR) of AvCoV (Callison et al., 2006) with the addition of a double Quencher. Amplification of the 143-bp fragment was performed in a 7500 Real Time PCR Cycler (Applied Biosystems™, CA, USA) using the following primers and probes (IDT, Iowa, USA): 5′ UTR forward primer, 5′-GCT TTT GAG CCT AGC GTT-3′; 5′ UTR reverse primer, 5′-GCC ATG TTG TCA CTG TCT ATT-3′; 5′ UTR probe, 5′-/5HEX/CA CCA CCA G/ZEN/A ACC TGT CAC CTC/3IABkFQ/-3′.

2.5. cDNA synthesis and sequencing

The spike glycoprotein gene region was amplified from qRT-PCR-positive samples. Briefly, cDNA was synthesised using a High Capacity cDNA Reverse Transcription kit (Applied Biosystems™, CA, USA). Next, a nested RT-PCR assay was performed using the following primers in the first step to amplify a 572-bp fragment: forward primer S7 5′-TACTACTACCAGAGTGC(C/T)TT-3′ and reverse primer S6 5′-ACATC(T/A)TGTGCGGTGCCATT-3′. The following primers were used in the second step to amplify a 530-bp fragment: forward primer S9 (5′-ATGGTTGGCATTT(A/G)CA(C/T)GG-3′) and reverse primer S5 (5′-GTGCCATTGACAAAATAAGC-3′) (Bochkov et al., 2007). This assay was performed in an Eppendorf MasterCycler®Pro S (NY, USA).

The amplified PCR products were purified using the MiniElute PCR Purification kit (QIAGEN, CA, USA) and quantified using an Epoch spectrophotometer (Biotek, Vermont, USA). Purified PCR products were sequenced by the Central Laboratory of High Performance Technologies in Life Sciences (LaCTAD/UNICAMP, São Paulo, Brazil). Sequencing reactions were performed using the Big Dye® Cycle Sequencing Terminator 3.1 kit (Applied Biosystems™, CA, USA) following the instructions provided by the manufacturer. The 3730XL DNA Analyser (Applied Biosystems™, CA, USA) platform was used for sequencing.

2.6. Sequence data collection and phylogenetic analyses

All bioinformatics and phylogeny experiments were performed using the Linux Cluster from the High Performance Computer Center, University of Florida, USA (UF HPC). For the bioinformatics and phylogenetic analyses, all available AvCoV spike 1 gene (S1) sequences from different animals were downloaded from the GenBank database (http://www.ncbi.nlm.nih.gov/genbank/) (Supplementary Table S2) and filtered using the following criteria: known sampling year; unknown sampling year; and known sampling year and isolation source (Fig. 2). Spike 2 gene regions (S2), clones, patents, and any recombinant sequences were excluded. Additionally, different CoV sequences were downloaded to represent CoVs from the genera *Alpha*, *Beta*, *Gamma*, and *Delta*. The

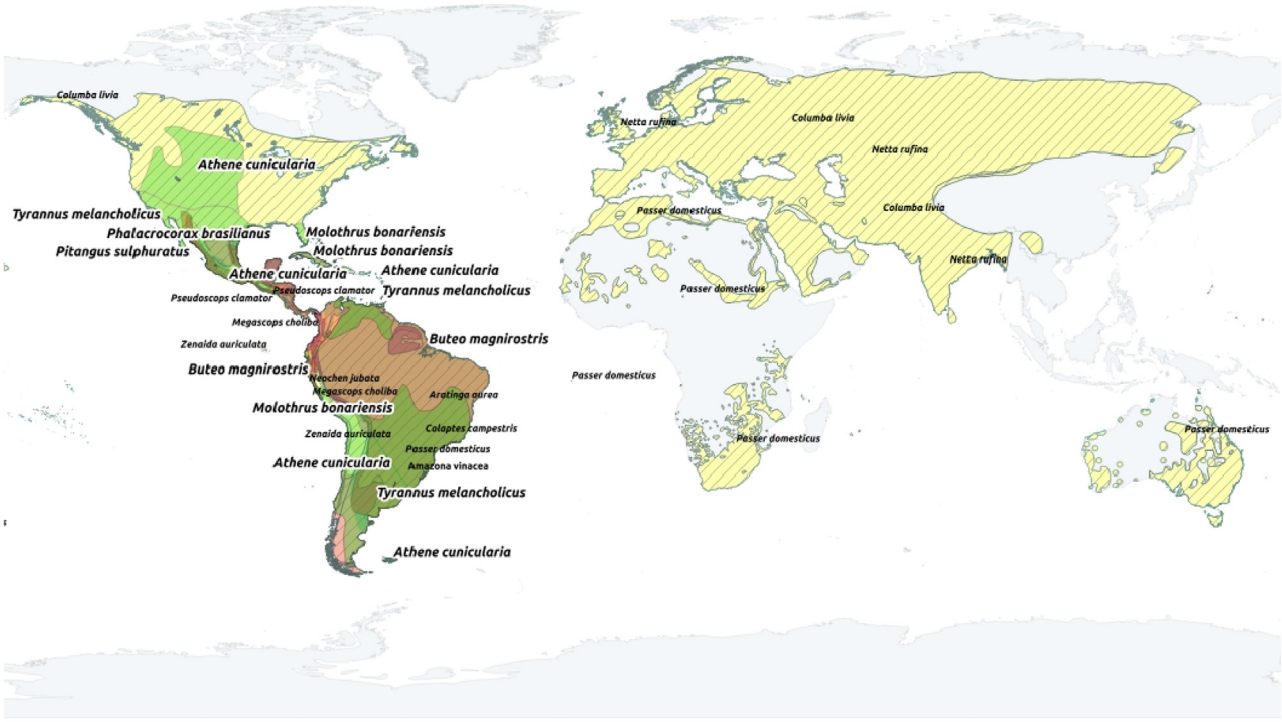

Fig. 1. Distribution map of migratory and non-migratory birds assessed in this study. The colours represent the specific region ranges in which the birds are present. The highlighted names indicate birds that participate in migration events. (For interpretation of the references to colour in this figure legend, the reader is referred to the web version of this article).

alignment was conducted using the parallel implementation of software ClustalW-MPI (Message Passing Interface) (Li, 2003).

The initial phylogenetic analyses were performed using Maximum Likelihood (ML) implemented in RAxML v.8 (Stamatakis, 2014) and FastTree v.2.1.7 (Price et al., 2010) software and the Relaxed Neighbour-Joining (RNJ) method in Clearcut software using the Kimura correction for pairwise distances (Sheneman et al., 2006). The ML analysis in RAxML was conducted using the general time reversible (GTR) + G and in FastTree using the standard implementation GTR + CAT with 20-parameter gamma optimisation and a mix of nearest-neighbour interchanges (NNI) and sub-tree-prune-regraft (SPR) for the tree topology search. ML tree reliability was analysed using bootstrap support (for RAxML) and Shimodaira–Hasegawa test (SH-like) (for FastTree) values with 1000 replicates (Anisimova and Gascuel, 2006); both methods compare the likelihood values of the best and second-best alternative arrangements around the branch of interest (Véras et al., 2011).

Two different ML tree construction software programmes were used to assess the potential for different clustering patterns of the sequences sampled from this study with the AvCoV S1 sequences downloaded from the GenBank database. Figtree v.1.4.2 (http://tree.bio.ed.ac.uk/software/figtree/) and OneZoom (Rosindell and Harmon, 2012) were used to visualise the large ML tree (file in the Supplementary Material). After the large ML tree was obtained, clades with node reliability ≥90% were selected using Phylopart to select sequences with high bootstrap values for Bayesian analysis (Prosperi et al., 2011).

2.7. Bayesian approach

Bayesian inference was performed using BEAST v.2.1.3 software (Bouckaert et al., 2014) assuming a strict or relaxed (uncorrelated Exponential and Log-Normal) molecular clock with different coalescent tree priors (constant population size, exponential growth, and Bayesian Skyline Plot (BSP)) (Drummond et al., 2005). Markov Chain Monte Carlo (MCMC) was executed with 450 million generations and sampled every 45,000 MCMC steps. Alternatively, LogCombiner v.2.1.3 (available in the BEAST v.2.1.3 package; http://beast.bio.ed.ac.uk/logcombiner) was used to resample the posterior distribution states at a lower frequency. The BEAST output files were analysed in Tracer v.1.6 with 10% burn-in (Rambaut et al., 2013). The Effective Sample Size (ESS) was ≥500 for each parameter assayed. Next, TreeAnnotator v.2.1.2 software (available in the BEAST v.2.1.3 package; http://beast.bio.ed.ac.uk/treeannotator) was used to produce maximum clade credibility (MCC) trees from each coalescent parameter. The trees were visualised in the graphical viewer Figtree v.1.4.2. Densitree software (Bouckaert et al., 2014) was used for density and qualitative analyses of the trees. The evolution models implemented were indicated by jModelTest v.2 software (Santorum et al., 2014).

Reconstruct Ancestral State in Phylogenies (RASP) v.2.1 software was used to infer biogeographical histories through the Bayesian Binary MCMC method (BBM) to predict biogeographical ancestral ranges with multiple MCMC iterations (Yu et al., 2014). The MCMC chains were run for five million generations, and the state was sampled every 100 generations. The analyses were performed under the Fixed JC + G (Jukes-Cantor + Gamma) model and the BBM with null root distributions.

2.8. Molecular clock analysis

The tMRCA and the evolutionary rate (assuming the nucleotide substitution per site per year) were inferred in the sequences designated as Clade 1 (representing wild and synanthropic birds) and Clade 2 (representing chickens) using BEAST v.2.1.3. Each sequence from Clades 1 and 2 was selected for the runs assuming the strict and relaxed molecular clock as described above. The nucleotide substitution models implemented in jModelTest v.2 were the GTR (Clade 1) and HKY (Clade 2). The relaxed (for Clade 1) and strict (for Clade 2) molecular clocks with the coalescent constant,

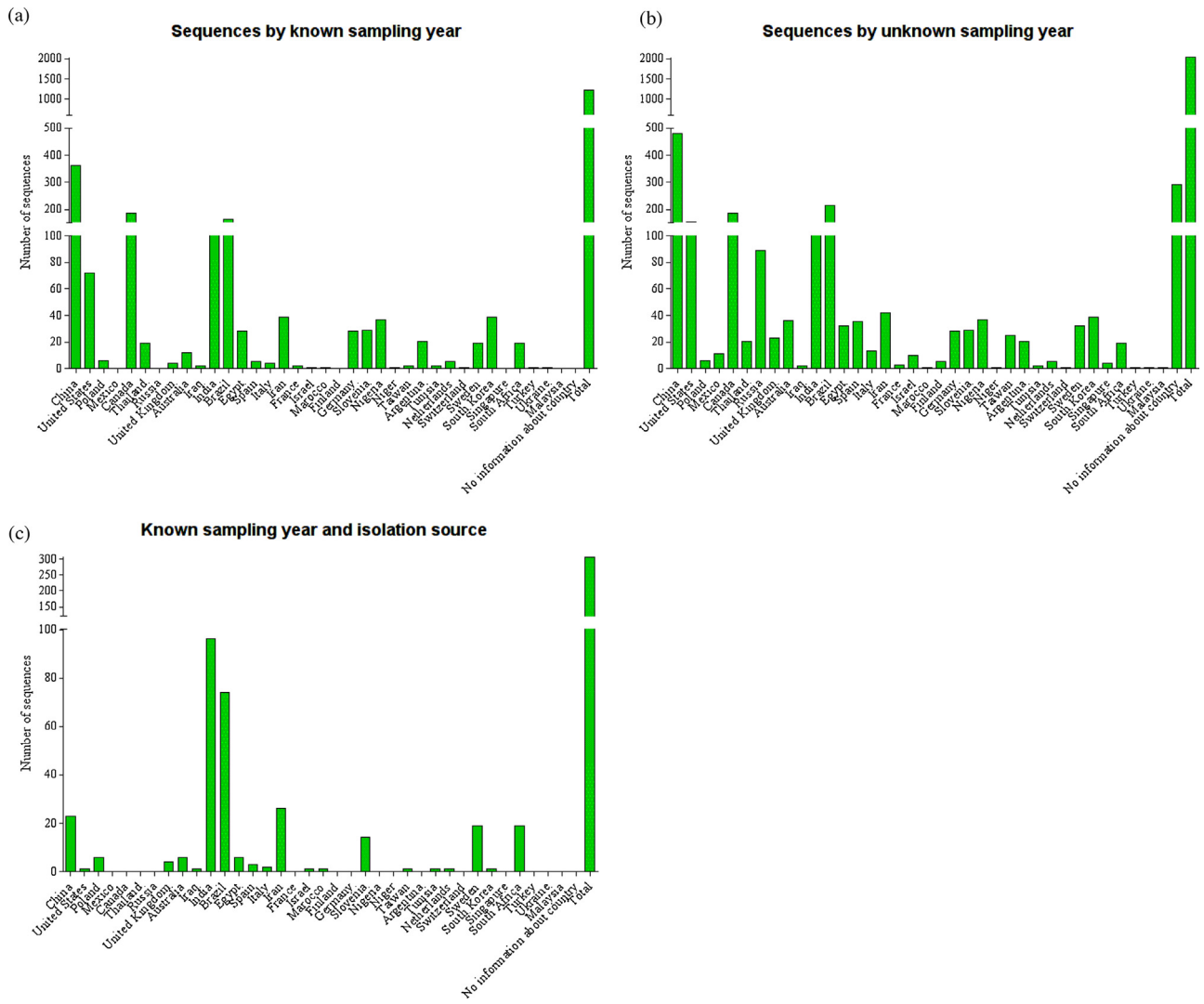

Fig. 2. AvCoV S1 gene sequences retrieved from GenBank and classified by (a) known sampling year, (b) unknown sampling year, and (c) known sampling year and isolation source.

exponential populations and BSP priors were used for Clade 1 analysis, while the BSP coalescent prior was used for Clade 2 analysis. The MCMC was performed with 450 million generations and sampled every 45,000 MCMC steps. The ESS was ≥500 for each parameter assayed to permit sufficient mixing between the Markov chain. Tracer v1.6 software was used to visualise the results.

2.9. Parsimony analysis

To trace the history of reconstruction of character states at ancestral nodes, a parsimony analysis was performed using the Mesquite v.2.75 software package (Maddison and Maddison, 2011). These analyses enabled the interpretation of the evolution of the various characteristics of the AvCoV strains and their evolutionary behaviour given a group of AvCoV organisms (Supplementary Fig. S1).

2.10. Bayesian phylogeography analysis

Evolutionary history parameters, including the evolution time of the AvCoV strains and their spatial and temporal dispersion, were estimated using the Bayesian phylogeography framework implemented in the BEAST v.2.1.3 software package (Bouckaert et al., 2014). To adjust the time scale of the trees, sequence data were obtained from the GenBank database and organised by specific criteria (see item 2.6). To accommodate variation between strains, a molecular clock approach (described above) was used to estimate ancestral spatial locations along the phylogenetic history. The results were analysed using the Tracer v.1.6 and TreeAnnotator v.2.1.2 software.

3. Results and discussion

3.1. AvCoV prevalence and phylogenetic analysis

Samples collected from 42 species of birds were tested for the presence of the 5′ UTR of AvCoV by real time RT-qPCR. Of these, 65 samples were positive (13.0%), including 43 (8.6%) tracheal and 22 (4.4%) cloacal swabs. AvCoV was detected in 22 different bird species distributed in 10 orders and 13 bird families. Among bird families, the virus was detected in *Anatidae* (3 of 10 species), *Ardeidae* (1 of 3 species), *Cathartidae* (1 of 1 species), *Columbidae* (3 of 3 species), *Falconidae* (1 of 2 species), *Icteridae* (1 of 1 species), *Passeridae* (1 of 1 species), *Phalacrocoracidae* (1 of 1 species), *Picidae* (1 of 1 species), *Psittacidae* (3 of 5 species), *Ramphastidae* (1 of

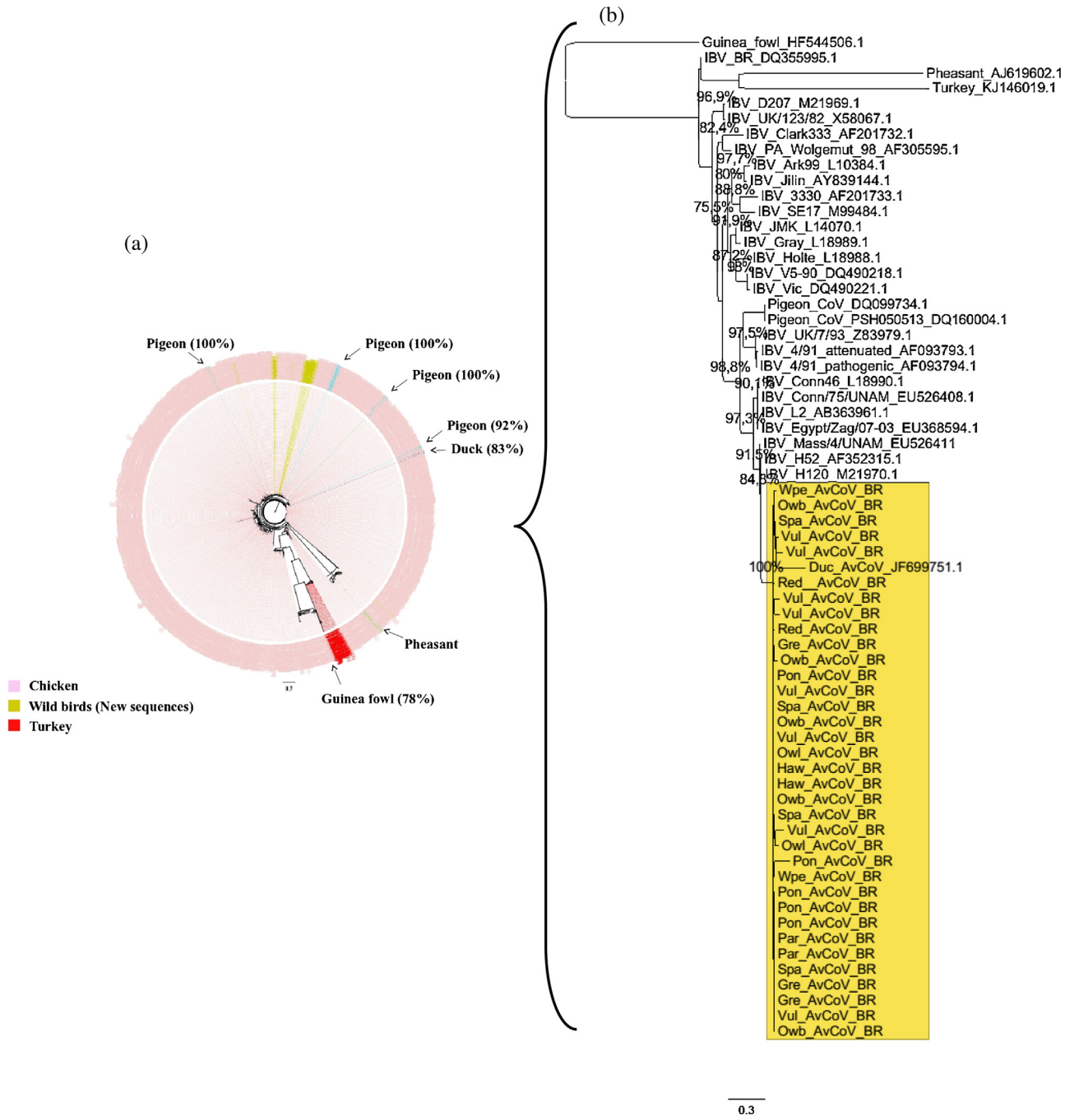

Fig. 3. ML phylogenetic trees of AvCoV S1 gene sequences from AvCoVs detected in different animals. Phylogenetic inference using 2079 AvCoV S1 gene sequences; each colour represents different species of birds, and the arrows indicate the positions of the birds in the tree (a). Phylogenetic inference from the large ML tree highlighting the sequences obtained in the study in greater detail (b). The Shimodaira–Hasegawa (SH-like) branch supports are shown on the trees. Only values greater than or equal to 75% are shown. Abbreviations: Pon, Pigeon; Vul, Vulture; Spa, Sparrow-Hawk; Owb, Owl bush; Owl, Owl; Wpe, Woodpecker; Gre, Great kiskadee; Par, Parrot; Red, Red-ruffed fruitcrow; Haw, Hawk; BR, Brazil. Only values greater than or equal to 75% are shown. (For interpretation of the references to colour in this figure legend, the reader is referred to the web version of this article).

1 species), *Strigidae* (3 of 3 species), and *Tyrannidae* (2 of 2 species) (Supplementary Table S3).

These findings reveal a high prevalence of AvCoVs circulating in birds other than chickens and suggest a potential role for wild and synanthropic birds as disseminators of AvCoVs in different avifaunas. These findings demonstrate that AvCoV is widespread in birds from the regions studied. Considering the economic and health impacts of AvCoV infections, the study of these viral agents has important implications for epidemiology as well as the elucidation of molecular ecology.

After detection of AvCoV and sequencing analysis, molecular evolution methods were used to phylogenetically characterise all positive samples. Analysis using an ML tree generated from 2079 S1 AvCoV sequences collected from pigeon and duck, guinea fowl and turkey sampled between 1956 and 2014 revealed a close phylogenetic relationship. By contrast, AvCoV sequences collected from wild birds in this study exhibited great divergence when compared with those detected in turkeys (Fig. 3). The same phylogenetic approach using the relaxed neighbour-joining method and an ML tree generated using RAxML software revealed similar patterns

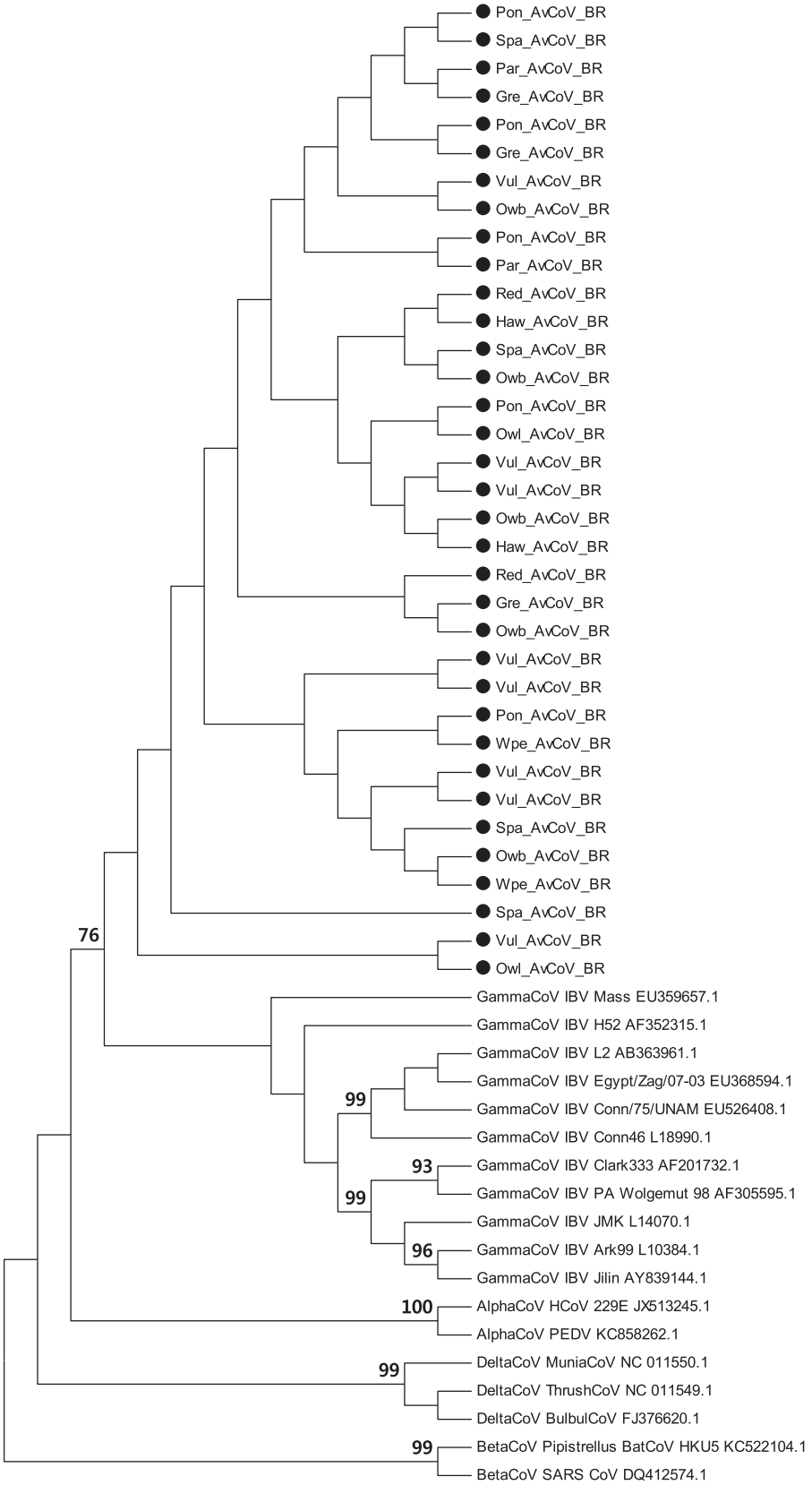

Fig. 4. Molecular phylogenetic analysis by the ML method with AvCoV S1 gene sequences from the *Alpha*, *Beta*, *Gamma*, and *Delta* CoV genera. Evolutionary history was inferred using the ML method based on the Kimura 2-parameter model. The black cycles represent the sequences collected in the study. The numbers above the branches indicate the bootstrap branch supports of 1000 replicates. Only values greater than or equal to 75% are shown. Abbreviations: Pon, Pigeon; Vul, Vulture; Spa, Sparrow-Hawk; Owb, Owl bush; Owl, Owl; Wpe, Woodpecker; Gre, Great kiskadee; Par, Parrot; Red, Red-ruffed fruitcrow; Haw, Hawk; BR, Brazil.

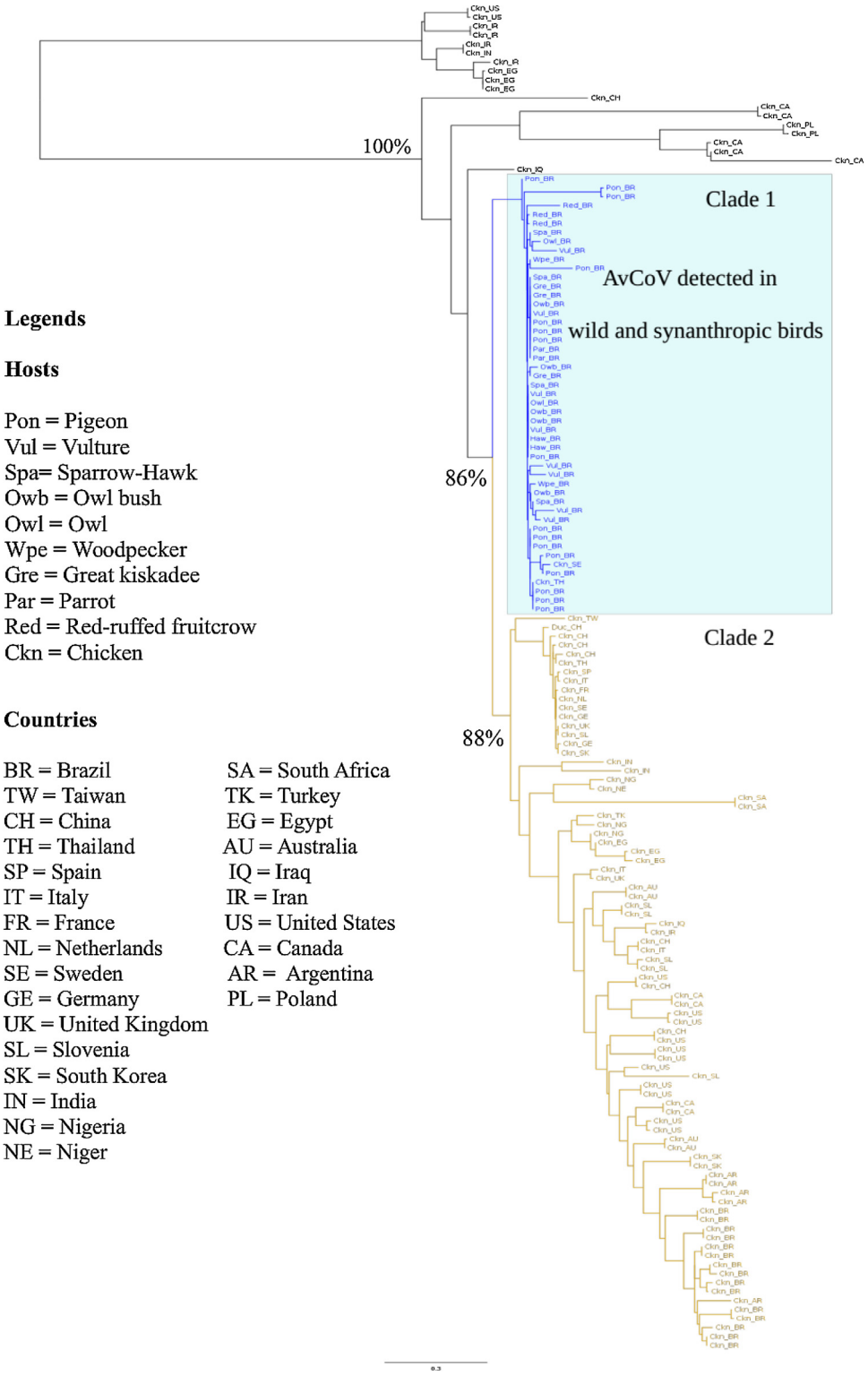

Fig. 5. ML phylogenetic tree of sequences from two well-supported clades extracted from the tree analysed in Fig. 3. Clade 1 (representing wild and synanthropic birds) and Clade 2 (representing chickens) are highlighted. The legends show the abbreviations of the animals and countries evaluated in the study. The numbers in the tree represent the Shimodaira–Hasegawa (SH-like) branch supports. Only values greater than or equal to 75% are shown.

of divergence and close relationships between species (data not shown). Then, a phylogenetic tree with the spike sequences from the *Alpha*, *Beta*, *Gamma* and *Delta* CoV groups was constructed to evaluate the representativity of the sequences from the study compared to the CoV sequences belonging to other CoV groups (Fig. 4).

Two well-supported clades was detected in the large ML tree. The first clade was designated Clade 1 and represents wild and synanthropic bird sequences (including two chicken sequences: one from Sweden (1999) (accession number JN022543.1) and one from Thailand (2008) (accession number GQ885131.1)). The second was designated Clade 2 and represents chicken sequences,

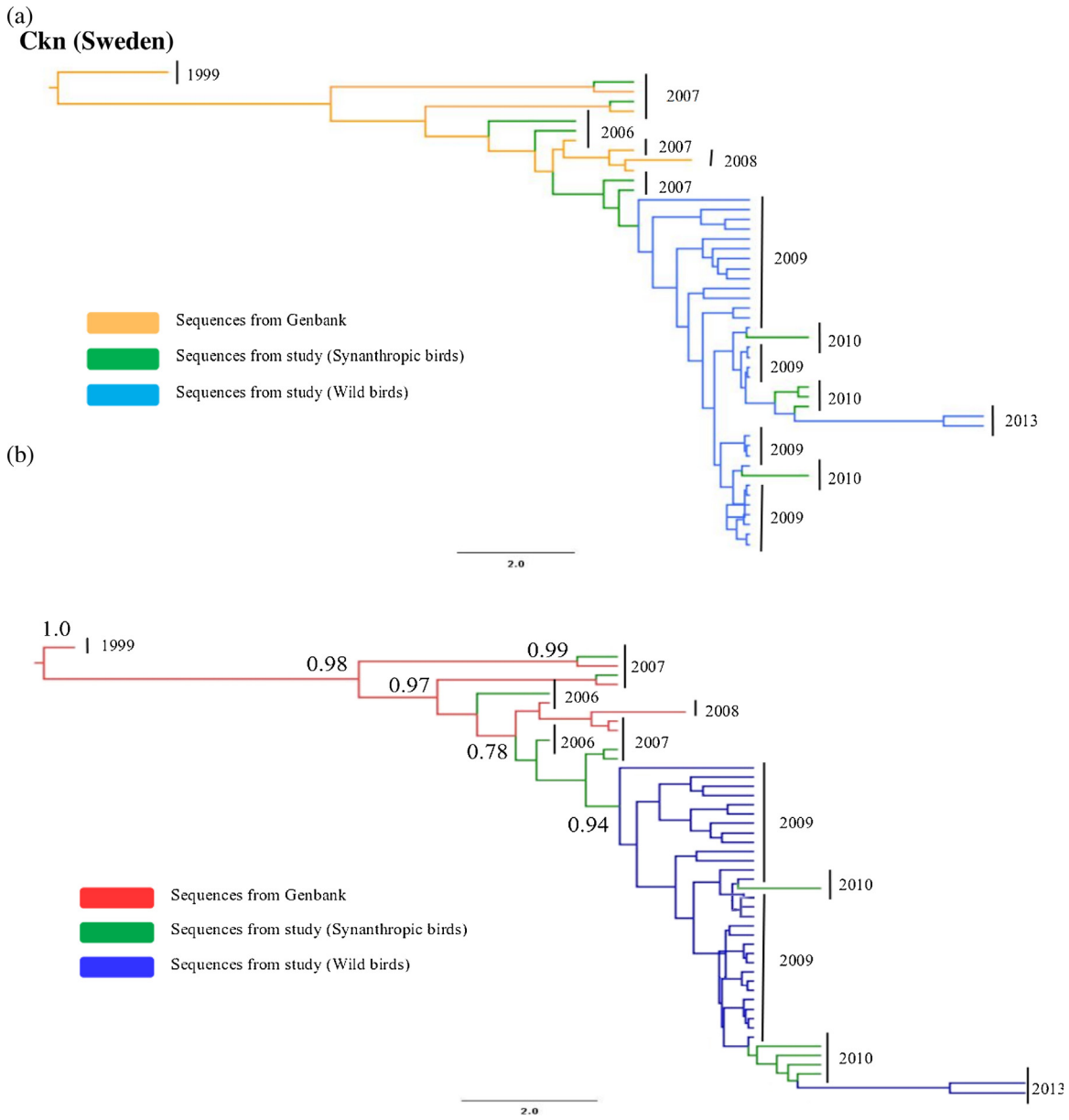

Fig. 6. MCC trees from Bayesian framework analysis of the AvCoV S1 gene. Data for the relaxed molecular clock for (a) coalescent constant population and (b) coalescent exponential population priors are shown. AvCoV sequences were collected from different animals. Obs.: Ckn (Sweden) indicates AIBV detected in a chicken from Sweden. The years preceding the branches indicate the collection date of the sequences. The posterior probability is represented by the numbers in the branches.

with the exception of a duck sequence from China collected in 2004 (accession number JF699751.1) (Fig. 5 and Supplementary Fig. S2).

3.2. *Tree topologies based on density and inference of biogeographic history (RASP)*

Because two clades were detected, a Bayesian approach using Densitree software was applied to verify the tree topologies based on the density of the stored trees (10,000 trees) from BEAST analysis. In this analysis, the branch with the strongest and densest colour was assumed to be the most likely tree topology. A chicken sequence from Sweden (1999) was observed as an outgroup in both coalescent priors models used (See Supplementary Fig. S3).

Based on the results of the Densitree software analysis described above, MCC trees were constructed by imposing a relaxed molecular clock. An AIBV strain from Sweden (1999) was inferred as the most recent common ancestor of the sequences collected in this study (Fig. 6 and Supplementary Fig. S4), suggesting that a strain collected 15 year ago may have been responsible for the emergence of new AvCoV strains in wild and synanthropic animals.

Following these analyses, the BBM framework was implemented to obtain a biogeographical reconstruction of the ancestral ranges of the AvCoVs detected in this study. First, ancestral nodes of AIBV from chickens were analysed. Ancestral nodes 78 (C, D, E, and F indicate a European ancestor), 80 (I, J, and L have a ancestral range from Australia, Canada, and South Korea), 92 (P and N have an ancestral range from Iraq and China) and 93 (O, P, and Q have an ancestral range from Slovenia, Italy, and Iraq) exhibit ambiguity and suggest the presence of two, three and four different reconstruction ancestral ranges (i.e., for each node analysed, there exists more than one biogeographic ancestor). In other words, the BBM analyses inferred two, three and four dispersal events involving countries on different continents (North America, Europe, Oceania, and Asia) (Fig. 7).

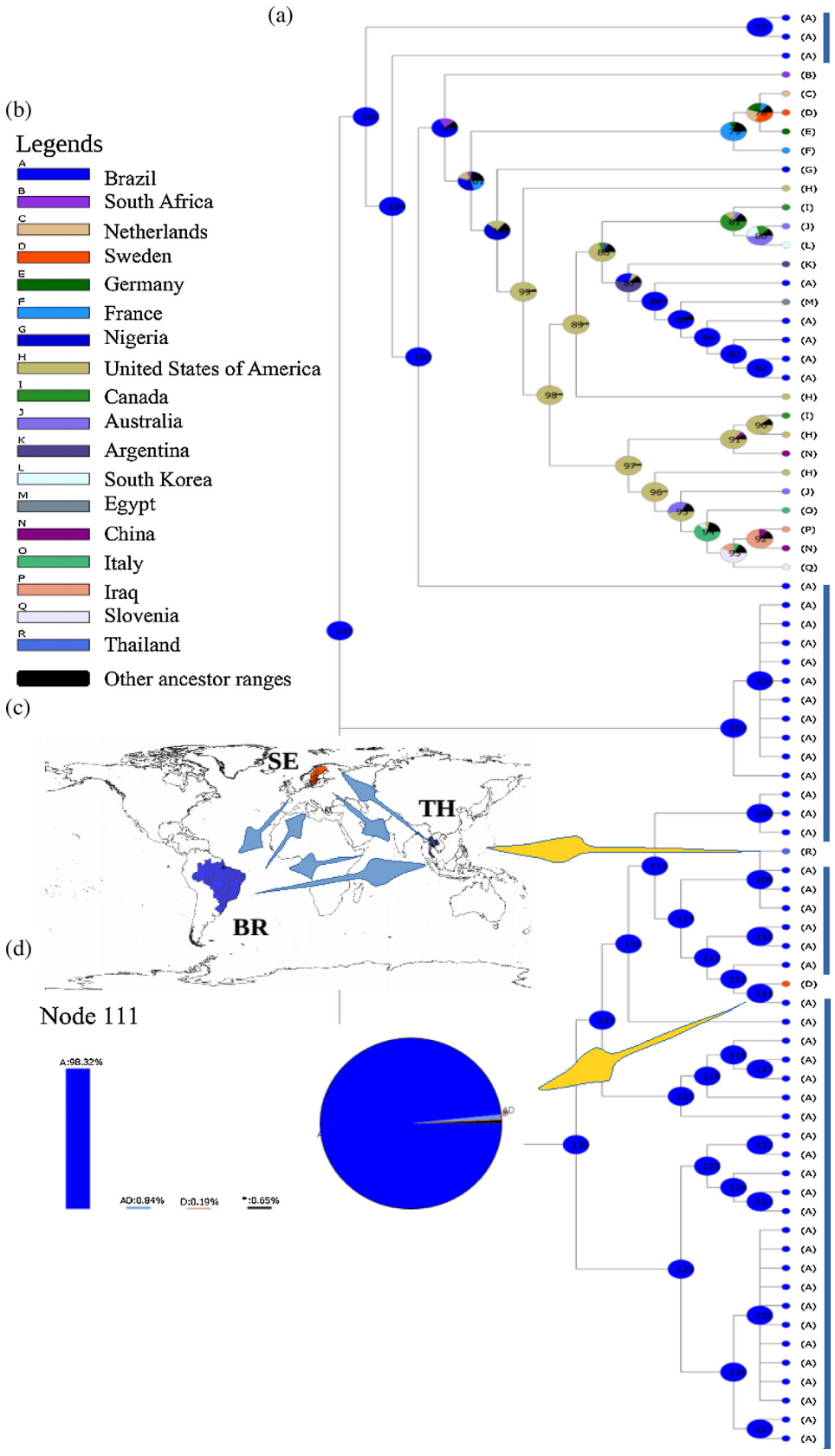

Fig. 7. Biogeographical ancestor reconstructions implemented in RASP software using the BBM method. Graphical results for the ancestral distributions at each node obtained from the phylogenetic analyses of AvCoV strains by BBM analysis. (a) RASP area reconstructions. (b) Each colour followed by a letter abbreviation represents a specific country assuming the possible ancestral ranges for the different nodes. The blue traces in the trees are the sequences collected in this study. The probabilities of alternative ancestral ranges are shown in pie charts at each node. (c) Possible route of the AvCoV strain from the host bird to the Brazilian birds assessed in the study. (d) Results from ancestral distributions at node 111 showing the percentage of ancestral identity between Swedish and Brazilian virus. Yellow arrows highlight the results from 111 and 109 ancestral nodes. Abbreviations: BR, Brazil; SE, Sweden; TH, Thailand. (For interpretation of the references to colour in this figure legend, the reader is referred to the web version of this article).

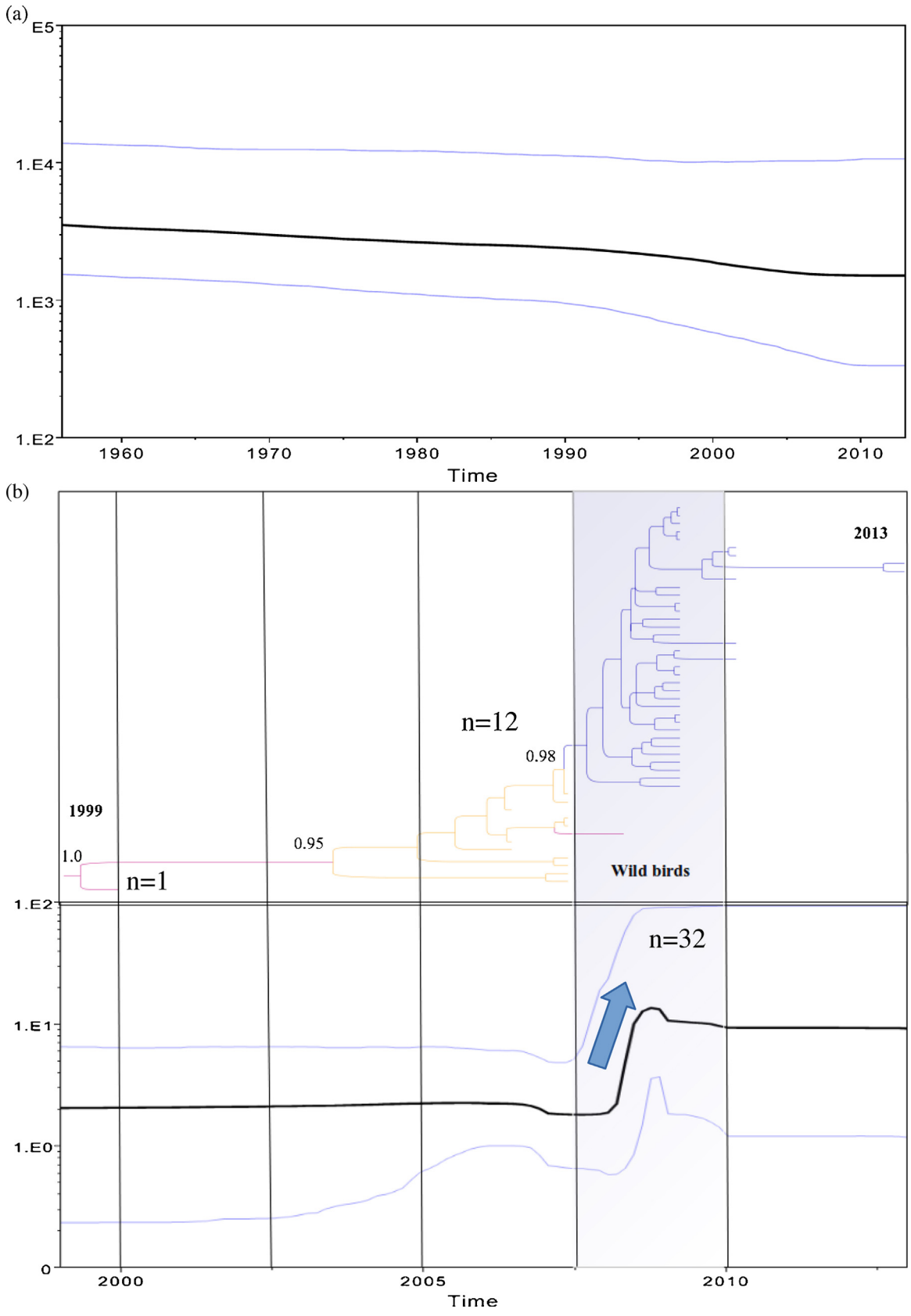

Fig. 8. BSP reconstruction of AvCoV strains detected in chickens (a) and in wild and synanthropic birds (b). Purple branches, chicken sequences; Yellow branches, pigeon sequences; Blue branches, sequences from wild birds. *N*, number of transmissions between different bird species. The blue arrow represents the increase in transmission between different bird species. The effective number of the population is represented on the *Y*-axis. Time is represented on the *X*-axis. Black lines indicate the medians and blue lines the credibility based on 95% highest posterior density (HPD) intervals. (For interpretation of the references to colour in this figure legend, the reader is referred to the web version of this article).

BBM analyses of the ancestral ranges of AvCoV strains from wild and synanthropic birds (highlighted with blue traces) revealed that most strains had only Brazilian identity. However, ancestral nodes 109 (A and R) and 111 (A and D) had a biogeographic ancestrality range from other countries. Data from the MCC trees showed that an AIBV strain from Sweden detected in chickens was the nearest ancestor; based on Node 111, the ancestrality frequency was 0.84% (AD), 0.19% (D), and 0.64% (from another ancestor range) (Fig. 7). From these analyses, our results suggest that wild birds may play a role in the spreading of AvCoVs amongst poultry around the globe.

3.3. Molecular clock analysis

The molecular clock hypothesis was evaluated for AvCoV strains using the likelihood ratio test (LRT) (Posada and Crandall, 1998), which compares the likelihood values of the topology assuming and not assuming the molecular clock. The time of divergence of the sequences from Clade 1 (AvCoV detected in wild and synanthropic birds) and 2 (AIBV sampled from chickens) was estimated, and the evolutionary rates for the sequences from Clade 1 and Clade 2 were calculated at 1.59×10^{-2} and 2.21×10^{-4} substitutions per site per year, respectively (Supplementary Table S4). The sequences from Clade 2 followed the molecular clock model according to the CoV evolutionary rate (Jackwood et al., 2012). Previous studies have estimated an evolutionary rate of $0.3–0.6 \times 10^{-2}$ for some AIBV strains (Cavanagh et al., 1998). Because the sequences were obtained from wild and synanthropic birds and AIBV is primarily found in chickens, we would expect to obtain a different result (i.e., strains from different environments may exhibit differences in evolutionary rates).

A high rate of CoV evolution leads not only to the generation of a diversity of strains and genotypes of CoV species but also to new species that can adapt to new hosts and ecological niches (Woo et al., 2009). Recent studies have identified CoV isolates from peacock (*Pavo cristatus*), partridge (*Alectoris* sp.), Guinea fowl (*Numida meleagris*) and teal (*Anas* sp.) with AIBV-like genomic characteristics (Liu et al., 2005; Chu et al., 2011). In addition, close contact between infected and susceptible animals facilitates the transmission of RNA viruses between species when two hosts are closely evolutionarily related (Cavanagh, 2005), as is the case for chickens and quails, which belong to the *Phasianidae* family.

3.4. Reconstruction of the demographic history

To reconstruct the demographic history and analyse past population growth over time, the BSP method was applied by enforcing the relaxed (Clade 1 sequences, AvCoV detected in wild and synanthropic birds) and strict (Clade 2 sequences, AIBV sampled from chickens) molecular clocks. This analysis demonstrated a constant and stationary equilibrium in demographic chicken populations over time (1956–2014, sequences from Clade 2) (Fig. 8A). Interestingly, the BSP reconstruction of the demographic history of AvCoV revealed an exponential increase in effective population size in 2009 (sequences from Clade 1) (Fig. 8B). An MCC tree from the BSP prior was positioned with the BSP graphic to verify data reproducibility. The results suggested that the potential increase of AvCoV strains in wild birds was directly related to the increase in animal interspecies AvCoV transmission ($n = 1$ to $n = 12$ to $n = 32$) (Fig. 8B). Use of the coalescent parameter from the exponential population growth model to observe the direction of viral transmissibility using the MCC tree approach (chicken ($n = 1$) to pigeon ($n = 12$) to wild birds ($n = 32$)) enabled an estimation of a coherent epidemiological trace for interspecies AvCoV transmission (Fig. 8B).

The frequency of viral transmission from birds to different hosts is increasing, and the viruses are gaining the ability to infect animals of different species, including the human population (e.g., the H1N1, H2N2, and H3N2 pandemic influenza viruses), either by viral evolutionary mechanisms that result in a new viral variant or via contact with different hosts. The main sources of new human viral diseases are enzootic and epizootic animal viruses (Parrish et al., 2008), and thus an in-depth phylogenetic and phylogeographic examination of the epidemiological context of AvCoV genetic diversity is extremely important.

This study employed an in-depth phylogenetic approach, and the results may be extended not only to understand the molecular dynamics of AvCoV evolution in different animals but also to other epidemiologically important pathogens. The emergence of new viral variants requires a better understanding of the molecular eco-epidemiology of these viral agents, which will require additional data regarding viral evolutionary behaviour, given the broad transmission and dissemination ranges of AvCoVs and CoVs in general. Finally, due the shortage of scientific studies applying in-depth bioinformatics and phylogenetic approaches in the AvCoV field and considering that many studies that detected CoVs in wild birds were conducted in recent years, a sudden expansion of AvCoVs has emerged in the public domain. Thus, some of the conclusions might be due to sampling bias.

Acknowledgements

The authors thank BirdLife International, Cambridge, United Kingdom, and NatureServe, Arlington, United States of America (2013), for providing the Geographic Information System (GIS) shapefiles of the bird species assessed in the study. This work was supported by FAPESP (Fundação de Amparo à Pesquisa do Estado de São Paulo-Brazil, grant 2011/50919-5 and 2013/03922-6) and CNPq (grant 311779/2014-0).

Appendix A. Supplementary data

Supplementary data associated with this article can be found, in the online version, at http://dx.doi.org/10.1016/j.virusres.2015.03.002.

References

Carstens, E.B., 2010. Ratification vote on taxonomic proposals to the International Committee on Taxonomy of Viruses. Arch. Virol. 155, 133–146, http://dx.doi.org/10.1007/s00705-009-0547-x.

Jackwood, M.W., Hall, D., Handel, A., 2012. Molecular evolution and emergence of avian gammacoronaviruses. Infect. Genet. Evol. 12, 1305–1311, http://dx.doi.org/10.1016/j.meegid.2012.05.003.

Fauquet, C.M., Mayo, M.A., Maniloff, J., Desselberger, U., Ball, L.A., 2005. Virus Taxonomy, VIII edition. Elsevier Academic Press, Amsterdam, pp. 937–955.

Mardani, K., Noormohammadi, A.H., Hooper, P., Ignjatovic, J., Browning, G.F., 2008. Infectious bronchitis viruses with a novel genomic organization. J. Virol. 82, 2013–2024, http://dx.doi.org/10.1128/JVI.01694-07.

Mo, M.L., Li, M., Huang, B.C., Fan, W.S.F., Wei, P., Wei, T.C., Cheng, Q.Y., Wei, Z.J., Lang, Y.H., 2013. Molecular characterization of major structural protein genes of avian coronavirus infectious bronchitis virus isolates in Southern China. Viruses 5, 3007–3020, http://dx.doi.org/10.3390/v5123007.

Cavanagh, D., Gelb, J., 2008. Infectious bronchitis. In: Saif, Y.M., et al. (Eds.), Diseases of Poultry. , 12th edition. Blackwell Publishing, Ames, IA, pp. 117–135.

Jones, R.C., 2010. Viral respiratory diseases (ILT, aMPV infections, IB): are they ever under control? Br. Poultry Sci. 51, 1–11, http://dx.doi.org/10.1080/00071660903541378.

Domanska-Blicharz, K., Jacukowicz, A., Lisowska, A., Wyrostek, K., Minta, Z., 2014. Detection and molecular characterization of infectious bronchitis-like viruses in wild bird populations. Avian Pathol. 43, 406–413, http://dx.doi.org/10.1080/03079457.2014.949619.

Keesing, F., Belden, L.K., Daszak, P., Dobson, A., Harvell, C.D., Holt, R.D., Hudson, P., Jolles, A., Jones, K.E., Mitchell, C.E., Myers, S.S., Bogich, T., Ostfeldet, R.S., 2010. Impacts of biodiversity on the emergence and transmission of infectious diseases. Nature 468, 647–652, http://dx.doi.org/10.1038/nature09575.

Jourdain, E., Gauthier-Clerc, M., Bicout, D.J., Sabatier, P., 2007. Bird migration routes and risk for pathogen dispersion into Western Mediterranean Wetlands. Emerg. Infect. Dis. 13, 365–372, http://dx.doi.org/10.3201/eid1303.060301.

Felippe, P.A., da Silva, L.H., Santos, M.M., Spilki, F.R., Arns, C.W., 2010. Genetic diversity of avian infectious bronchitis virus isolated from domestic chicken flocks

and coronaviruses from feral pigeons in Brazil between 2003 and 2009. Avian Dis. 54, 1191–1196, http://dx.doi.org/10.1637/9546-937110-DIGEST.1.
Somveille, M., Manica, A., Butchart, S.H.M., Rodrigues, A.S.L., 2013. Mapping global diversity patterns for migratory birds. PLoS ONE 8, 1–10, http://dx.doi.org/10.1371/journal.pone.0070907.
Lemey, P., Rambaut, A., Drummond, A.J., Suchard, M.A., 2009. Bayesian phylogeography finds its roots. PLoS Comput. Biol. 5, 1–16, http://dx.doi.org/10.1371/journal.pcbi.1000520.
Yang, Z., Rannala, B., 2012. Molecular phylogenetics: principles and practice. Nat. Rev. Genet. 13, 303–314, http://dx.doi.org/10.1038/nrg3186.
Holmes, E.C., 2004. The phylogeography of human viruses. Mol. Ecol. 13, 745–756, http://dx.doi.org/10.1046/j.1365-294X.2003.02051.x.
Kühnert, D., Wu, C.H., Drummond, A.J., 2011. Phylogenetic and epidemic modeling of rapidly evolving infectious diseases. Infect. Genet. Evol. 11, 1825–1841, http://dx.doi.org/10.1016/j.meegid.2011.08.005.
Callison, S.A., Hilton, D.A., Boyton, T.O., Sample, B.P., Robison, R., Swayne, D.E., Jackwood, M.W., 2006. Development and evaluation of a real-time Taqman RT-PCR assay for the detection of infectious bronchitis virus from infected chickens. J. Virol. Methods 138, 60–65, http://dx.doi.org/10.1016/j.jviromet.2006.07.018.
Bochkov, Y.A., Tosi, G., Massi, P., Drygin, V.V., 2007. Phylogenetic analysis of partial S1 and N gene sequences of infectious bronchitis virus isolates from Italy revealed genetic diversity and recombination. Virus Genes 35, 65–71, http://dx.doi.org/10.1007/s11262-006-0037-0.
Li, K.B., 2003. ClustalW-MPI: ClustalW analysis using distributed and parallel computing. Bioinformatics 19, 1585–1586, http://dx.doi.org/10.1093/bioinformatics/btg192.
Stamatakis, A., 2014. RAxML Version 8: a tool for phylogenetic analysis and post-analysis of large phylogenies. Bioinformatics 30, 1312–1313, http://dx.doi.org/10.1093/bioinformatics/btu033.
Price, M.N., Dehal, P.S., Arkin, A.P., 2010. FastTree 2—approximately maximum-likelihood trees for large alignments. PLoS ONE 5, 1–10, http://dx.doi.org/10.1371/journal.pone.0009490.
Sheneman, L., Evans, J., Foster, J.A., 2006. Clearcut: a fast implementation of relaxed neighbor joining. Bioinformatics 22, 2823–2824, http://dx.doi.org/10.1093/bioinformatics/btl478.
Anisimova, M., Gascuel, O., 2006. Approximate likelihood-ratio test for branches: a fast, accurate, and powerful alternative. Syst. Biol. 55, 539–552, http://dx.doi.org/10.1080/10635150600755453.
Véras, N.M.C., Gray, R., Brígido, L.F.M., Rosângela, R., Salemi, M., 2011. High-resolution phylogenetics and phylogeography of human immunodeficiency vírus type 1 subtype C epidemic in South America. J. Gen. Virol. 92, 1698–1709, http://dx.doi.org/10.1099/vir.0.028951-0.
Rosindell, J., Harmon, L.J., 2012. OneZoom: a fractal explorer for the tree of life. PLoS Biol. 10, 1–5, http://dx.doi.org/10.1371/journal.pbio.1001406.
Prosperi, M.C.F., Ciccozzi, M., Fanti, I., Saladini, F., Pecorari, M., Borghi, V., Giambenedetto, S.D., Bruzzone, B., Capetti, A., Vivarelli, A., Rusconi, S., Re, M.C., Gismondo, M.R., Sighinolfi, L., Gray, R.R., Salemi, M., Zazzi, M., Luca, A.D., 2011. A novel methodology for large-scale phylogeny partition. Nat. Commun. 2, 321, http://dx.doi.org/10.1038/ncomms1325.
Bouckaert, R., Heled, J., Kühnert, D., Vaughan, T., Wu, C.H., Xie, D., Suchard, M.A., Rambaut, A., Drummond, A.J., 2014. BEAST 2: a software platform for Bayesian evolutionary analysis. PLoS Comput. Biol. 10, 1–6, http://dx.doi.org/10.1371/journal.pcbi.1003537.
Drummond, A.J., Rambaut, A., Shapiro, B., Pybus, O.G., 2005. Bayesian coalescent inference of past population dynamics from molecular sequences. Mol. Biol. Evol. 22, 1185–1192, http://dx.doi.org/10.1093/molbev/msi103.
Rambaut, A., Suchard, M., Drummond, A.J., Available: http://tree.bio.ed.ac.uk/software/tracer/Accessed 20 June 2014 2013. MCMC Trace Analysis Package.
Santorum, J.M., Darriba, D., Taboada, G.L., Posada, D., 2014. jmodeltest.org: selection of nucleotide substitution models on the cloud. Bioinformatics 30, 1310–1311, http://dx.doi.org/10.1093/bioinformatics/btu032.
Yu, Y., Harris, A.J., He, X.J., Available at http://mnh.scu.edu.cn/soft/blog/RASP 2014. RASP (Reconstruct Ancestral State in Phylogenies) 3.0.
Maddison, W.P., Maddison, D.R., Available online at: http://mesquiteproject.org 2011. Mesquite: A Modular System for Evolutionary Analysis. Version 2.75.
Posada, D., Crandall, K.A., 1998. Modeltest: testing the model of DNA substitution. Bioinformatics 14, 817–818, http://dx.doi.org/10.1093/bioinformatics/14.9.817.
Cavanagh, D., Mawditt, K., Adzhar, A., Gough, R.E., Picault, J.P., Naylor, C.J., Haydon, D., Shaw, K., Britton, P., 1998. Does IBV change slowly despite the capacity of the spike protein to vary greatly? Adv. Exp. Med. Biol. 440, 729–734, http://dx.doi.org/10.1007/978-1-4615-5331-1_94.
Woo, P.C.Y., Lau, S.K.P., Lam, C., Lai, K.Y., Huang, Y., Lee, P., Luk, G., Dyrting, K.C., Chan, K., Yuen, K., 2009. Comparative analysis of complete genome sequences of three avian coronaviruses reveals a novel group 3c Coronavirus. J. Virol. 83, 908–917, http://dx.doi.org/10.1128/JVI.01977-08.
Liu, S., Chen, J., Chen, J., Kong, X., Shao, Y., Han, Z., Feng, L., Cai, X., Gu, S., Liu, M., 2005. Isolation of avian infectious bronchitis coronavirus from domestic peafowl (*Pavo cristatus*) and teal (*Anas*). J. Gen. Virol. 86, 719–725, http://dx.doi.org/10.1099/vir.0.80546-0.
Chu, D.K.W., Leung, C.Y.H., Gilbert, M., Joyner, P.H., Ng, E.M., Tse, T.M., Guan, Y.i., Peiris, J.S.M., Poon, L.L.M., 2011. Avian coronavirus in wild aquatic birds. J. Virol. 85, 12815–12820, http://dx.doi.org/10.1128/JVI.05838-11.
Cavanagh, D., 2005. Coronaviruses in poultry and other birds. Avian Pathol. 34, 439–448, http://dx.doi.org/10.1080/03079450500367682.
Parrish, C.R., Holmes, E.C., Morens, D.M., Park, E.C., Burke, D.S., Calisher, C.H., Laughlin, C.A., Saif, L.J., Daszak, P., 2008. Cross-species virus transmission and the emergence of new epidemic diseases. Microbiol. Mol. Biol. Rev. 72, 457–470, http://dx.doi.org/10.1128/MMBR.00004-08.